A novel test rig for the dynamic characterization of large size tilting pad journal bearings

You may also be interested in:

Energy Harvesting for Aerospace Structural Health Monitoring Systems
M R Pearson, M J Eaton, R Pullin et al.

The effect of external dynamic loads on the lifetime of rolling element bearings: accurate
measurement of the bearing behaviour
W Jacobs, R Boonen, P Sas et al.

Dynamic characterization of the cutting conditions in dry turning
R Serra, H Chibane and R Leroy

Novel dynamic fatigue-testing device
Chee-Hoe Foong, Marian Wiercigroch and William F Deans

Dynamic characterization and modeling of magneto-rheological elastomers under compressive loadings
J H Koo, F Khan, D D Jang et al.

Characterizing the Peano fluidic muscle and the effects of its geometry properties on its behavior
Allan Joshua Veale, Sheng Quan Xie and Iain Alexander Anderson

High-Bandwidth Dynamic Full-Field Profilometry for Nano-Scale Characterization of MEMS
Liang-Chia Chen, Yao-Ting Huang and Pi-Bai Chang

A novel test rig for the dynamic characterization of large size tilting pad journal bearings

P Forte[1,2] **, E Ciulli**[1] **and D Saba**[1]

[1] Department of Civil and industrial Engineering, University of Pisa, Largo Lazzarino, 56122 Pisa, Italy

[2] p.forte@ing.unipi.it

Abstract. The present work concerns the realization of a test bench for the dynamic characterization of high performance tilting pad journal bearings, within a collaboration between the Department of Civil and Industrial Engineering of Pisa, GE Oil&Gas and AM Testing. The objective is to cover journal diameters of interest of GE, from 150 to 300 mm, with peripheral speeds up to 150 m/s, static load up to 270 kN, dynamic loads up to 30 kN and frequencies up to 350 Hz, performances that make the apparatus very competitive worldwide. The adopted configuration has the test article (TA) floating at the mid-span of a rotor supported by two rolling bearings. The TA is statically loaded by a hydraulic actuator and excited dynamically by two orthogonal hydraulic actuators. Construction was recently concluded and preliminary tests are under way. In order to assess in advance the possible accuracy of the tests, a dynamic lumped parameter model of the test bench was developed to perform virtual experiments, including several possible sources of experimental errors and uncertainties. The model was implemented using reduced stiffness and mass matrices obtained from Finite Element Analysis by Component Modal Synthesis.

1. Introduction
Tilting pad journal bearings (TPJB) are commonly used in turbomachinery for their characteristics of stability at high rotational speeds. Due to their influence on the dynamic behavior of the rotor, their theoretical modeling and experimental characterization is essential in the design phase of the machine.

According to the classical analytical approach [1] the dynamic behavior of a journal tilting pad bearing is determined by n+2 degrees of freedom, namely the two degrees of freedom that describe the motion of the journal center in the transverse plane and the rotations of the n pads. The hydrodynamic forces exerted by the fluid on the rotor are non-linear functions of the position and speed of the rotor and of the various pads.

About the equilibrium configuration, these functions are approximated by linear relationships by using matrices of stiffness and damping coefficients. For the calculation of the dynamic coefficients the perturbation approach or numerical differentiation are applied and the assembly of the single pad matrices yields the entire bearing matrix. Finally, the assumption of synchronous pad rotation brings to a formulation of the dynamic equilibrium dependent only on the rotor degrees of freedom and to reduced matrices of the dynamic coefficients, 2x2, with the main diagonal composed of direct coefficients and the secondary diagonal of cross-coupled coefficients.

So, if **u** is the vector of the lateral displacements of the shaft relative to the stator and **f** the vector of the corresponding forces, the following relation can be written

$$\boldsymbol{f} = \boldsymbol{H}\,\boldsymbol{u} \tag{1}$$

where **H** is the complex matrix representing the bearing frequency response, called by some authors mechanical impedance [1-3]. Separating the real and imaginary parts,

$$\boldsymbol{H}(\omega) = \boldsymbol{K}(\omega) + i\omega\boldsymbol{C}(\omega) \tag{2}$$

where the matrices **K**, **C** are the stiffness and damping matrices dependent on frequency ω, and their elements are the dynamic stiffness and damping coefficients.

Traditional analysis does not consider thermal effects in their entirety and neglects the effects of turbulence, thermal expansion and pivot and pad elastic deformations. However, there are now closed ad hoc codes [4], based on the equation of Reynolds and on different formulations of the energy equation, that claim to include these aspects in the analysis.

In order to validate the theoretical models different test stands have been constructed over the years [5]. The dynamic coefficients of the bearing in the frequency domain are estimated on the basis of the dynamic loading (harmonic forces, impulsive or random) applied on the rotor or on the bearing housing and the relative rotor/stator displacements. The most common test bench configuration is the one that provides the test bearing floating at mid-span of a fixed rotor supported by two rolling bearings. The bearing is loaded statically and it is dynamically excited by two independent actuators in two orthogonal directions. The main laboratories adopting the fixed rotor and floating stator configuration are: 1) Turbomachinery Lab, Texas A&M University, USA [6], 2) Department of Mechanical and Aerospace Engineering, University of Virginia, USA [7,8], 3) NRC, Ottawa, Canada and Kingsbury, 4) Power and Industrial System R&D Center, Toshiba Corporation, Yokohama, Japan [9], 5) Research and Development Centre, HANJUNG, Korea [10], 6) Doosan Heavy Industries & Construction and Pusan National University, Korea [11]. The solutions of the various laboratories have quite different performances. In particular: a) the rotor diameter ranges from a minimum of 70 mm of the University of Virginia to a maximum of 580 of Toshiba, b) the maximum rotor speed is achieved by Kingsbury (128 m/s) c) the maximum specific load on the bearing by the Texas A&M University (3100 kPa), d) the maximum applicable load by NRC Ottawa (25000 N), e) the maximum driver power by Toshiba (2400 kW), f) the maximum flow rate by Toshiba (774 l/min). Less common is the configuration of two identical fixed test bearings (100 mm diameter) that support the rotor free to move like a real configuration (Polytechnic of Milan) [2].

Despite the complexity of the codes, the percentage difference between the numerical and the experimental results is not always negligible for the direct stiffness and damping coefficients, and is generally significant for the cross-coupled ones [5,12] especially for conditions out of the common ranges of size and operation. That justifies the effort of developing a new test facility for the dynamic characterization of high performance tilting pad journal bearings to extend the ranges of test parameters and support the development of complete lines of products for turbomachinery of industrial interest.

The work presented here is the result of a collaboration between the Department of Civil and Industrial Engineering of the University of Pisa, GE Oil&Gas and AM Testing within the ATENE project (Advanced Technologies for ENergy Efficiency) funded by the Tuscany Region. The test bench design will be outlined and its key issues discussed. In addition, a dynamic lumped parameter model, developed to simulate experiments and to assess in advance the possible accuracy of the tests, will be presented.

2. Test bench

2.1. Test bench requirements

Based on the state of the art and the needs of GE Oil&Gas, the requirements on the test facility were defined with the fundamental aim of allowing full scale bearing static and dynamic characterization tests. The test facility had to be versatile and allow tests on bearings of diameter D = 150-300 mm, with axial length to diameter ratio L/D = 0.4-1.0, peripheral velocity (V_p) up to 150 m/s, with a maximum specific load of 3 MPa and a constant temperature of the oil supply, from 60 to 120°C. The values of speed and pressure correspond to a maximum rotation speed of about 20000 rpm for the smaller diameter (150 mm) and at a maximum load of about 270 kN for the major diameter (300 mm) with L/D = 1. It was not required that all extremes were met simultaneously but consistent with the maximum available power for the test bench and the auxiliary systems that is about 1 MW. In table 1 the required values of torque, power and oil flow rate are reported.

Table 1. Required torque (T), power (P) and oil flow rate (Q)

	Vp (m/s)	D=150 mm			D=300 mm		
		T (Nm)	P (kW)	Q (l/min)	T (Nm)	P (kW)	Q (l/min)
L/D=1	150	140	280	300	-	-	-
	130	115	200	270	-	-	-
L/D=0.4	150	63	125	150	390	390	950
	130	49	85	130	306	265	800

2.2. The test cell

Due to the size of the bearing, the test bench has a floating bearing configuration (figure 1).
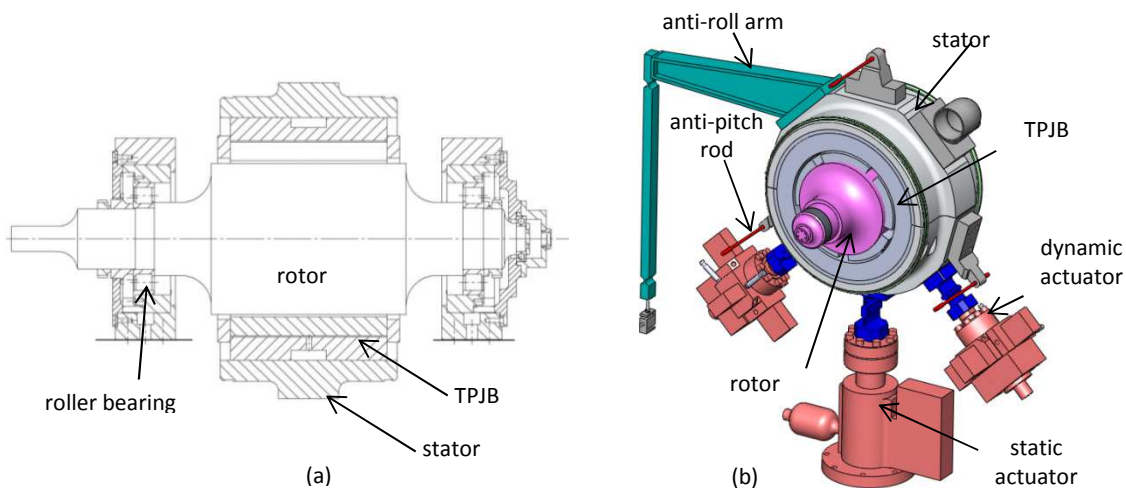

Figure 1. Test cell: (a) rotor group, (b) actuators and stator constraints.

The TAs are provided with the same external diameter so that they can be housed in the same stator bushing, divided in two halves to ease mounting and dismounting of the TA. The stator bushing is made of steel because simulations have highlighted the need to stiffen the cylindrical wall to reduce ovalization under load and possible measurement errors.

Given the TA size range, manufacturing of one rotor for each TA diameter was found more convenient. The rotor is made of a single steel solid having a central part of the TA diameter and the two end journals of the diameter of the bench bearings (figure 1a). The shaft shoulder fillet is large to limit the stress concentration factor and also to increase shaft stiffness. As for the latter aspect, a 280 mm diameter shaft. for instance, has a mid-span deflection of 0.075 mm for a load of 235 kN.

The analysis of the shaft bearing characteristics highlighted the need to select a different type for each diameter of the TA. That means providing a pair of supports divided into two halves to allow mounting of bearings of quite different size by means of interface bushings. Due to the high loads and speeds involved, aeronautical high precision roller bearings were selected.

Three "anti-pitch rods" constrain the stator to move in the vertical plane perpendicular to the rotor axis and prevent longitudinal motion and pitching (figure 1b). They have been dimensioned so as to have a flexural stiffness of less than 0.1% of the TA minimum direct stiffness coefficient. An "anti-roll arm" prevents the rotation of the stator about the longitudinal axis but not its translatonal motion; the reaction exerted on the stator, though small due to the length of the arm, is not neglected and is measured by a load cell.

The static load on the TA is applied by means of a hydraulic actuator in the vertical direction upwards to operate against the force of gravity and realize the condition of zero load without inversion of the applied force. The actuator, equipped with a pressurized gas accumulator, is also sufficiently compliant not to interfere with the dynamic actuators. The alternating forces are mutually orthogonal, at 45° with respect to the vertical direction. This choice was due to the fact that the structure of the test system is symmetrical with respect to the longitudinal vertical plane passing through the axis of the rotor and that the stiffness of the TA is considerably higher in the direction of the static load. With this arrangement two identical actuators can be employed working simultaneously in phase to obtain the vertical force and in antiphase to provide the horizontal force, with a significant benefit on sizing. Even in this case hydraulic actuators were selected because, while presenting significant limitations in performance as frequency increases, they allow to reach high values of load with acceptable size and mass. In particular through-rod piston cylinders, each served by 4-high dynamic servo valves, were selected. The use of multiple servo-valves in parallel is necessary because at high frequency only 25% of maximum opening is guaranteed.

Each actuator should ideally act in the direction of its axis without generating cross-reactions. The practical impossibility to comply with this requirement by means of ideal mechanical hinges has led to interposing stingers (figure 2) between the actuator and the stator, with high longitudinal stiffness, and much lower but not negligible transverse stiffness. The stinger axial stiffness is about 10^6 N/mm, comparable with the direct coefficients of stiffness of the TA while the transversal stiffness is 2 orders of magnitude smaller.
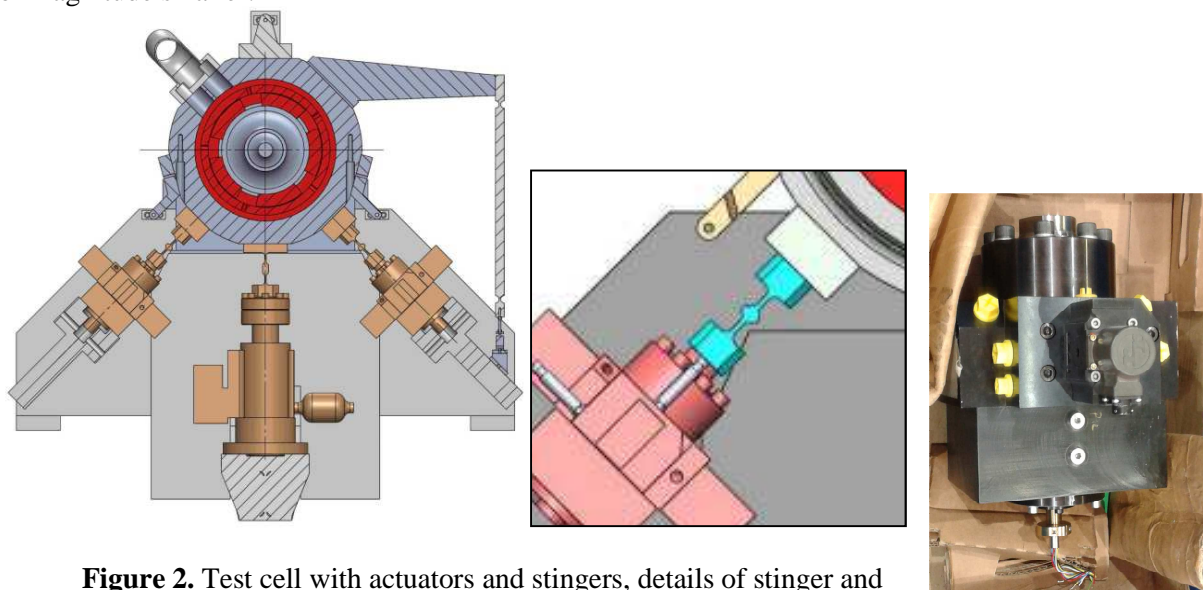

Figure 2. Test cell with actuators and stingers, details of stinger and dynamic actuator.

Another aspect to consider is the stiffness of all the components of the test cell (rotor, stator, bearings, frame). Since the load path from the actuators on the stator of the bearing is closed through the frame and the rolling bearings supporting the rotor, the deformations of this system must be compatible with the stroke of the actuators and with the desired relative displacement between the rotor and the stator. Therefore, on the one hand, the actuators must be capable of developing an alternating displacement of at least 0.1 mm when exerting the maximum force at the maximum frequency and, on the other, the components of the test section must be very stiff. In particular, as regards the test cell frame (figure 3), the solution adopted envisages the use of two thick plates 120 mm connected by two cross members of 400x80 mm section. With this configuration, the deformation at the base of the actuators corresponding to the maximum load does not exceed 0.01 mm except for two resonance peaks in the frequency range of interest. In any case, an experimental dynamic characterization will be necessary to avoid resonance frequencies.
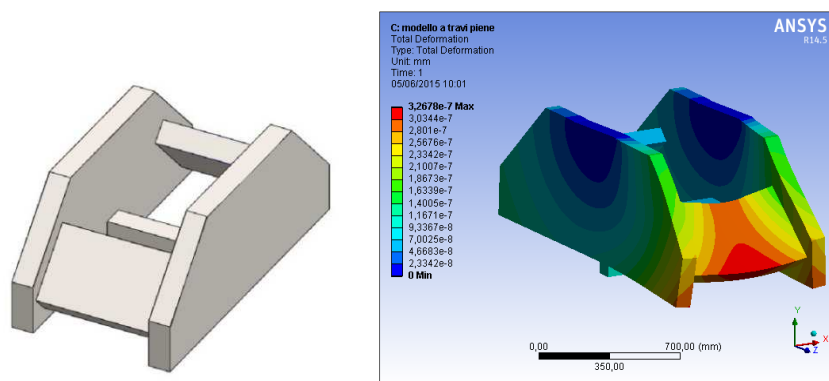

Figure 3. Test cell frame: solid model and FE analysis.

2.3. The test bench layout
Figure 4 shows the general layout of the test bench, with the test cell on the right and the motor and the multiplier gear box on the left.
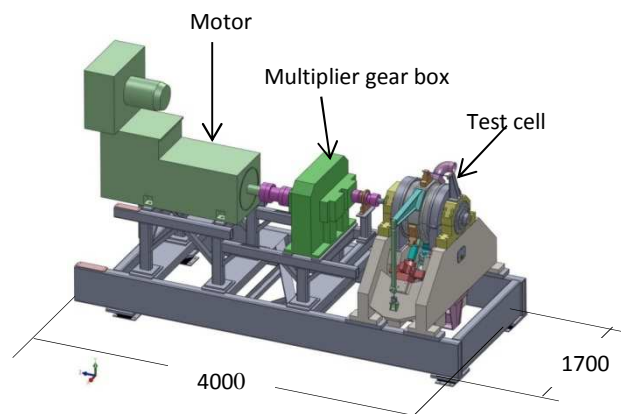

Figure 4. Test bench layout.

The rotor is driven by a 630 kW three-phase asynchronous motor controlled by an inverter. The maximum speed is 4000 rpm and the maximum torque 6300 Nm. The motor is connected by an elastic disc coupling to a single stage multiplier with herringbone gears and a gear ratio of 6:1. The gear output shaft is then connected to the rotor of the test cell by a torque meter (full scale 1 kNm).

The bench frame supporting and connecting the test section, the multiplier and the electric motor consists mainly of a longitudinal structure that supports the weight of the components straddling the

inground basin for the oil tank. The frame is provided with anti-vibration pads. A second structure allows the vertical alignment of the axes of the three groups.

Of utmost importance is the analysis of the resonances of the bench frame in the frequency range of interest. To reduce the problem of vibrations, a frame made of beams with hollow rectangular section that can be filled with granular material to dissipate energy and limit the frequency response was conceived.

2.4. The lubrication system

The lubrication system, is equipped with storage tank of about 4000 l, positioned below the test bench, inside a basin 460x300 cm large, and 100 cm deep. The oil flow rate is kept constant, with a maximum percentage deviation of ± 1% of the set value, within the range from 125 to 1100 l/min. The maximum pressure at the test cell inlet is 3 bar. The oil temperature at the test cell inlet is kept constant with a maximum deviation of 2°C compared to the set value, in the range 60 to 120°C.

The oil is conveyed into the TA by means of a tube, connected to the upper part of the stator where two holes allow the oil to reach the TA. The stator is also connected to two oil recovery sleeves through two lip seals. The system allows radial displacements of a few tenths of a millimeter with negligible forces, ensuring at the same time the oil confinement. These sleeves, running along the support plates of the rotor bearings, convey the oil in the tank below.

An additional lubrication system is necessary to supply the multiplier gear box while a high pressure system supplies the actuators.

Finally a suitable oil cooling system is provided to remove the power dissipated primarily in the TA, by means of cooling towers.

2.5. The measurement system

The sensors employed in this test bench to measure the quantities for the identification of the static and dynamic characteristics of the tested bearings, without considering those of the auxiliary systems, and that of the TA, instrumented by the client, are the following:

- proximity sensors and accelerometers
- force sensors
- torque meter with speedometer

High resolution proximity sensors, located at two cross-sections (two per section) of the stator and facing the cylindrical surface of the rotor, enable the measurement of relative displacements of the two components in two orthogonal directions. Similarly, four uniaxial acceleration sensors are also placed on the stator of the TA to measure acceleration in two planes and two orthogonal directions for the indirect measurement of the force of inertia. In each section there are also two sensors of lower precision in diametrically opposite position with respect to the main ones. These additional sensors are necessary to measure eccentricity and identify the point of stationary operation because the rotor diameter can vary due to centrifugal effects and thermal expansion.

The actuators are controlled by force. The stingers of the dynamic actuators are equipped with strain gauges to measure the radial and tangential forces applied to the stator. The load applied by the static actuator is measured through an integrated pressure sensor. A uniaxial load cell measures the anti-roll constraint reaction.

The speedometer is used to measure the rotation of the motor speed and, together with the torque meter, the instantaneous power absorbed by the rotor during the tests.

Finally, a control and data acquisition system is provided to set the test conditions and to acquire the signals of the several sensors installed on the bench and its auxiliary systems.

3. Test procedure

Each test is characterized by a point of steady state operation, defined by the shaft rotation speed, the static load and the lubricating oil flow rate, temperature and viscosity.

When steady state conditions are reached, the dynamic actuators impose multiple frequency sinusoidal forces in the frequency range of interest, typically below the synchronous frequency (below 20000 rpm, or 330 Hz). For the moment the actuators are planned to operate one at a time, thus imposing to the stator approximately rectilinear orbits, but in general any elliptical orbit is suitable for the purpose. The displacement amplitude must be sufficiently small to avoid the effects of non-linearity in the dynamic behavior of the bearing.

The sensor data are sampled at sufficiently high frequency, filtered to isolate the frequencies of excitation and frequency transformed. The Fourier transform of the force and displacement signals is the input data for the identification process of dynamic coefficients. Identical tests are repeated in rapid succession to decrease the effect of random errors on the sensor signals.

For the identification of the dynamic coefficients, with the assumption of linearity, two tests are required for each excitation frequency [6]. In fact by the matrix equation

$$\begin{bmatrix} f_{1x} & f_{2x} \\ f_{1y} & f_{2y} \end{bmatrix} = \begin{bmatrix} H_{xx} & H_{xy} \\ H_{yx} & H_{yy} \end{bmatrix} \begin{bmatrix} u_{1x} & u_{2x} \\ u_{1y} & u_{2y} \end{bmatrix} \tag{3}$$

it is possible to calculate the four dynamic coefficients knowing the relative displacements and the forces exchanged by the rotor and the stator. The relative displacements are measured by the proximity sensors, while for the exchanged forces only an indirect measure is available, given by the equilibrium equation

$$\boldsymbol{f} = \boldsymbol{f}_S - \mathbf{H}_I \boldsymbol{u}_S \tag{4}$$

where $\mathbf{f}_S$ is the resultant of the forces applied to the stator, measured by the force sensors, $\mathbf{u}_S$ are the stator displacements, measured by the accelerometers, and $\mathbf{H}_I$ represents the inertia of the stator.

The inertia of the stator can be calculated from CAD or measured by appropriate tests decoupling the rotor and the stator. They are performed without oil, by exciting the stator avoiding contact with the rotor. Because there is no exchange of forces between the rotor and the stator, equation (4) becomes

$$0 = \boldsymbol{f}_{S0} - \mathbf{H}_I \boldsymbol{u}_{S0} \tag{5}$$

that allows to obtain, with two tests, the inertial term.

4. Simulation of experiments

In order to check the effectiveness of the identification procedure and to evaluate the criticality of the measurement system a lumped parameter model able to simulate the dynamic behavior of the test cell was developed. The work flow is shown schematically in figure 5, where the modeling steps are distinct from the subsequent simulation phase.

The input data for the virtual experiment are the excitation forces (or displacements) on the hydraulic actuators. Some components of the model are available in interchangeable versions, so one can evaluate different case studies (different diameters or alternative design choices) and various simplifying assumptions in the model. In particular, the virtual experiment can be run with different TA in various test conditions.

The errors in the measures of individual sensors are estimated based on the characteristics of the sensor and the data acquisition system. Since all calculations are done in the frequency domain, what matters is the error in the measurement of amplitude and phase of the signal, that is the complex amplitude. A preliminary analysis will therefore provide a conservative estimate of the variance of the measurement error of the sensor. Errors in indirect measures are computed using the error propagation, assuming that errors in measures are independent of each other.

In addition to the errors of the sensors, the virtual experiment allows us to consider sources of systematic errors due to simplifications in the test procedure. A simplification derives from the fact that some forces are considered negligible and are not measured, for example, the shear forces exerted by the stabilizer bars. Another simplification concerns displacements and it is due to the assumption

that the stator and the rotor, where the position sensors are mounted, are considered as rigid bodies. Actually the deformations are generally not negligible and influence the measurement.
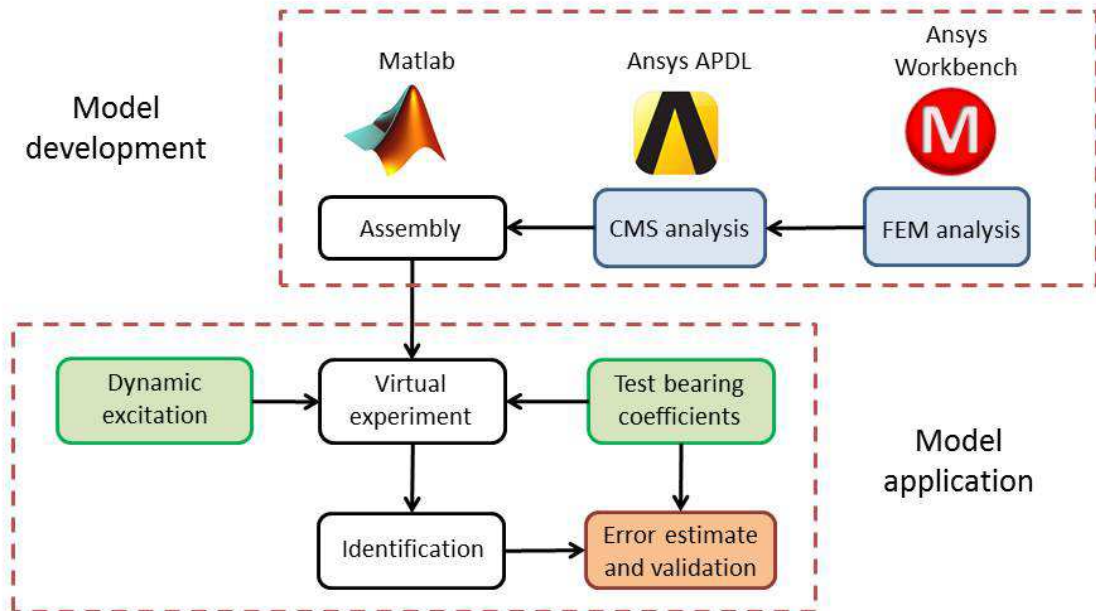

Figure 5. Work flow of modeling and simulation.

4.1. Lumped parameter model

The test cell has been divided into components, each of which was assigned a relatively small number of interface nodes. Figure 6 gives an example of decomposition into components, with highlighted interface nodes. The behavior of each component, reported to the nodes, is described by an impedance matrix.
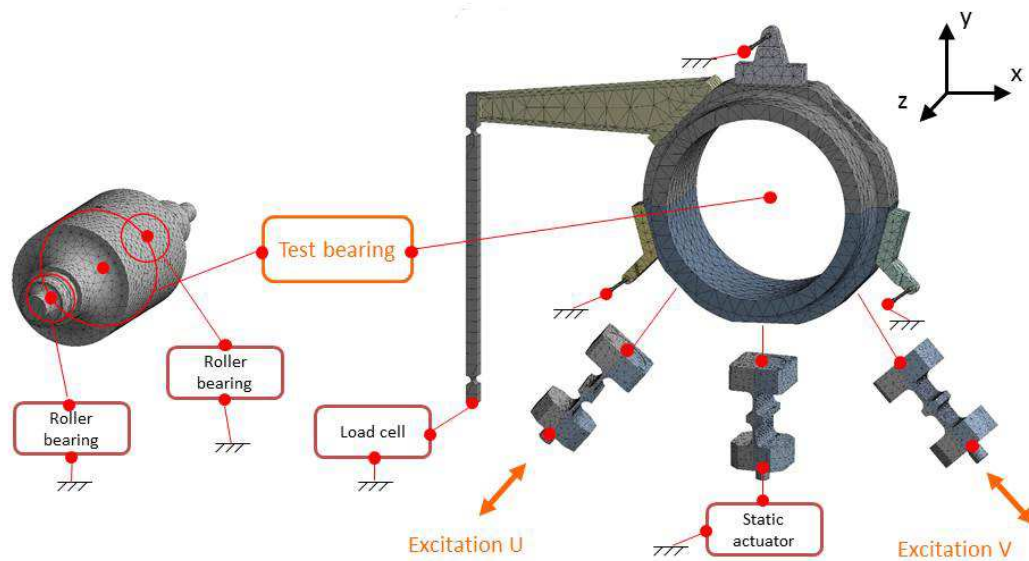

Figure 6. Interface nodes of the test cell components.

For some members the structural dynamic behavior is obtained from finite element analysis (FEM) using Component Modal Synthesis (CMS) [13] generating super-element stiffness, mass and damping matrices. The CMS method differs from the methods of static analysis sub-structuring for the presence of modal degrees of freedom that require a prior modal analysis. Since the maximum frequency of interest was 330 Hz the natural frequencies of modal analysis were truncated at 1000 Hz.

For other components the impedance matrix is built manually, starting from analytical calculations, as in the case of roller bearings, or by the technical data of the supplier, as in the case of the load cell of the anti-roll bar. In the case of rigid body models, adopted for some components, they are implemented as "multi-point constraints" using the method of Lagrange multipliers [14].

The global "lumped" model was obtained in MATLAB environment, following the standard procedure for the assembly of finite elements, namely by creating a map between the degrees of freedom of the elements and those of the assembly, and by adding the matrices of the stiffness, mass and damping of each component. The term "lumped" is used to emphasize that the discretization was pushed to the point of maintaining only a small number of degrees of freedom, chosen in advance, considered sufficient to describe the overall behavior of the system.

The interface nodes represented in figure 6 are used to connect the components of the model. Other interface nodes, not shown in the figure, simulate the position of sensors.

4.2. Results

The results reported in this paper refer to the simulation of an identification test performed considering a bearing of 300 mm diameter and 300 mm long, with 5 pads, load on pad. The static load was 40.5 kN. The dynamic load, applied by one actuator at a time, had an amplitude of 1 kN at each frequency. The shaft rotational speed was set at 7000 rpm and the dynamic coefficients introduced in the model of the TA are shown in table 2 (y is the direction of static load). Such values were defined by extrapolation on the basis of data of a smaller bearing calculated with a proprietary code made available by GE Oil&Gas. In any case, since the aim of the test was to verify the effectiveness of the identification procedure, the actual correspondence to real experimental values is not as important as the coefficient order of magnitude. 2% structural damping was added to components synthesized with CMS, directly in MATLAB environment.

Table 2. TA dynamic characteristics at 7000 rpm, synchronous frequency.

		xx	xy	yx	yy
Stiffness coefficients	K (N/m)	$4.91 \cdot 10^8$	$-4.51 \cdot 10^6$	$4.92 \cdot 10^6$	$5.35 \cdot 10^8$
Damping coefficients	C (Ns/m)	$4.60 \cdot 10^5$	$3.16 \cdot 10^3$	$-2.95 \cdot 10^3$	$4.68 \cdot 10^5$

4.2.1. Systematic errors. Among the performed analyses, a comparison was made between a model with an ideal rigid stator bushing and two models with flexible stator bushings (figure 6), of steel and aluminium respectively, to verify the effect of the deformability of the stator. If rigid, the TA bushing is also supposed rigid, while in the flexible cases the TA is assumed of steel. The pads are in any case considered rigid with concentrated mass and moments of inertia.

The elastic compliance of the journals is already included in the dynamic coefficients of the TA in table 2 and not in the stator model.

Figure 7 presents the plots of the TA stiffness coefficients and the three compared models. Note that in these simulations the stiffness and damping of the TA were assumed, for the sake of simplicity, independent of frequency and equal to the synchronous values.

From the plots one can see that, with a rigid stator bushing model, the test seems to give very small systematic errors that can be ascribed in large part to the flexibility of the rotor. Models with flexible

stator bushings show much larger systematic errors, especially in the horizontal direction, perpendicular to the static load.

This kind of systematic error can be explained with the ovalization deformations that affect the measurement because both proximity probes and accelerometers, are mounted on the stator bushing and measure radial displacements.
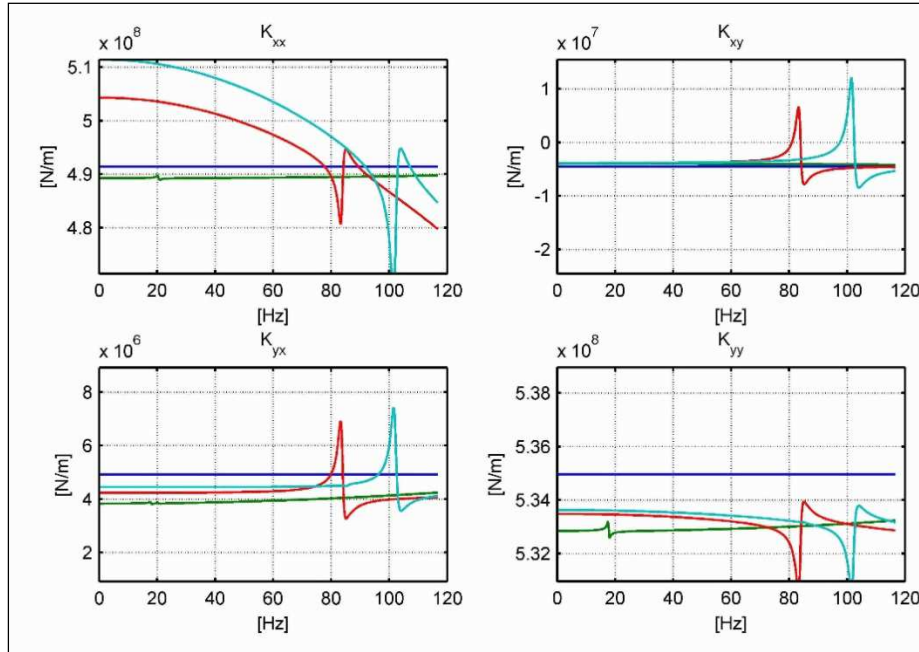

Figure 7. Systematic errors in the stiffness coefficients for the three models (blue-reference, green-rigid bushing, red-steel bushing, cyan-aluminum bushing).

It is important to note that the distribution of forces among the different pads significantly affects the deformations of the stator. Due to the difficulty of devising an accurate though simple model of the TA, the only statement that can be made for now is that ovalization effects are not negligible and it is advisable to stiffen the stator bushing.

4.2.2. Random errors. Starting from the estimate of sensor random errors, an estimate of the error in the dynamic coefficients can be achieved very simply. The identification procedure corresponds to a function

$$h = h(s) \tag{6}$$

that transforms sensor data **s** in dynamic coefficients **h**. Here we consider, **s** and **h** column vectors of real values, appropriately separating the real and imaginary parts of the complex values used in the previous sections. For small values of the errors, the relation (6) can be linearized and the propagation of errors is estimated by

$$\boldsymbol{V}_h = \boldsymbol{J}\,\boldsymbol{V}_s\boldsymbol{J}^{\mathsf{T}} \tag{7}$$

where $\boldsymbol{V}_s$ is the covariance matrix of the sensors, $\boldsymbol{V}_h$ that of the dynamic coefficients and $\boldsymbol{J} = \partial\boldsymbol{h}/\partial\boldsymbol{s}$ is the Jacobian transformation matrix.

Figure 8 shows the confidence limits defined on the basis of mean square error for the case of the rigid stator. The results for a dynamic load amplitude of 1 kN. are based on a very preliminary estimate of the uncertainty of the sensors, but still give an idea of the orders of magnitude. The

following standard deviations were assumed:, 0.1 μm for proximity sensors, 1g for accelerometers, 10 N for load cells.
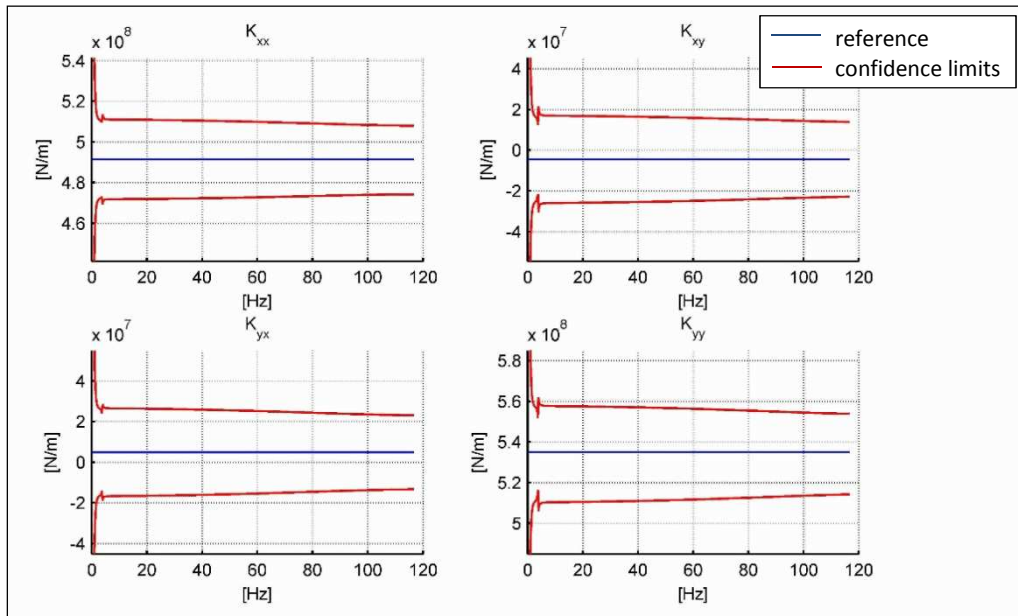

Figure 8. Random errors in dynamic stiffness coefficients

The confidence bounds may seem too large, but two issues should be considered. The first is that each measurement shall be repeated tens of times, so that the random error can be easily reduced of an order of magnitude. The second is that the amplitude of oscillation of 1 kN for the excitation forces is very precautionary. Doubling the excitation doubles oscillation amplitudes, halves position errors and roughly halves confidence bounds.

5. Conclusions

This paper presented a novel high-performance test bench for the characterization of hydrodynamic bearings of large size. The proposed test bench has an architecture similar to other existing ones but is definitely competitive, especially for maximum peripheral speed and oil flow, unique in its kind in Europe. Its performance is essentially limited by the maximum possible motor power and disposal of produced heat, with regards to logistics and financial resources. Its total cost was about 700 k€.

Particular attention was paid to the load application system that provides the maximum performance obtainable with hydraulic technology in terms of the force-displacement-frequency. Its limits at high frequencies and at high loads have led to the use of stingers for the connection with the casing of bearing to be tested and to stiffen all elements of the test section. This solution involves not negligible cross reactions to the load and the need for their measurement to be taken into account in the dynamic identification process of the bearing dynamic coefficients.

The test bench is in the commissioning phase. To support not only the development of the test bench but also the testing procedure and analysis of results, a simulation tool was developed to estimate the accuracy of the measurement and identification process. The estimates were made by running a virtual experiment which simulates the dynamic test apparatus and the identification procedure. The mechanical simulation is performed on a lumped parameter model obtained by making use of the CMS method to condense the dynamic behavior of the more complex structural components.

Results showed a critical issue due to the stator bushing flexibility, source of excessive errors on the measurement of the coefficients. That brought to choose steel rather than aluminum for the stator

preferring the maximum stiffness criterion instead of the minimum weight criterion. Moreover additional proximity sensors were provided to measure the extent of ovalization. In any case predictive corrections based on the dynamic model of the system can be introduced in the identification process.

As regards random errors, simulation indicated that in order to obtain acceptable confidence limits measurements should be repeated at least a few dozen times.

For each test article it will be necessary to define frequency content and amplitude of excitation loads and number of test repetitions but, once defined a cost function, the virtual experiment might be used to optimize the identification procedure, case by case.

References

[1]   Dimond T, Younan A and Allaire P 2011 A review of tilting pad bearing theory *Int. J. of Rotating Machinery* 908469

[2]   Chatterton S, Pennacchi P, Vania A, Tanzi E and Ricci R 2011 Characterization of five-pad tilting-pad journal bearings using an original test-rig *Proc. ASME DETC2011 (Washington)* 48166

[3]   Géradin M and Rixen D J 2015 *Mechanical vibrations: theory and application to structural dynamics* 3rd ed (John Wiley & Sons)

[4]   He M and Allaire P 2003 Thermoelastohydrodynamic analysis of fluid film journal bearings *UVA Report* UVA/643092/MAE03/595

[5]   Dimond T W, Sheth P N, Allaire P E and He M 2009 Identification methods and test results for tilting pad and fixed geometry journal bearing dynamic coefficients – A review *Shock and Vibration* **16** 13–43

[6]   Childs D W and Hale K 1994 A Test Apparatus and Facility to Identify the Rotordynamic Coefficients of High-Speed Hydrostatic Bearings *ASME Journal of Tribology* **116** 337–344

[7]   Wygant K, Flack R D and Barrett L E 2004 Measured Performance of Tilting Pad Journal Bearings over a Range of Preload – Part. I: Static Operating Conditions *STLE Tribology Transactions* **47** 576-584

[8]   Wygant K, Flack R D and Barrett L E 2004 Measured Performance of Tilting Pad Journal Bearings over a Range of Preload – Part. II: Dynamic Operating Conditions *STLE Tribology Transactions* **47** 585-593

[9]   Ikeda K, Hirano T, Yamashita T, Mikami M and Sakakida H 2006 An Experimental Study of Static and Dynamic Characteristics of a 580 mm (22.8 in.) Diameter Direct Lubrication Tilting Pad Journal Bearing *ASME Journal of Tribology* **128** 146

[10]   Ha H C and Yang S H 1999 Excitation Frequency Effects on the Stiffness and Damping Coefficients of a Five-Pad Tilting Pad Journal Bearing *ASME Journal of Tribology* **121** 517

[11]   Bang K B, Kim J H and Cho Y J 2010 Comparison of power loss and pad temperature for leading edge groove tilting pad journal bearings and conventional tilting pad journal bearings *Tribology International* **43** 1287–1293

[12]   Delgado A, Vannini G, Ertas B, Drexel M and Naldi L 2011 Identification and Prediction of Force Coefficients in a Five-Pad and Four-Pad Tilting Pad Bearing for Load-on-Pad and Load-Between-Pad Configurations" *J. Eng. Gas Turbines and Power* **133**(9) 9 p

[13]   Craig R R 1987 A review of time-domain and frequency domain component-mode synthesis methods *Int. J. Anal. and Exp. Modal Analysis* **2**(2) 59-72

[14]   Belytschko T, Liu W K, Moran B and Elkhodary K I 2014 *Nonlinear finite elements for continua and structures* 3rd ed (John Wiley & Sons)